ECS Solid State Letters, **1** (3) P48-P50 (2012)
2162-8742/2012/1(3)/P48/3/$28.00 © The Electrochemical Society

Double-Pattern Textured ZnO:Ga Thin Films Fabricated by an APPJ and an DC Sputtering

Shu-Hung Yu,[a,z] Po-Ching Ho,[a,*] Teng-Wei Yang,[a] Chien-Chung Bi,[b] Chih-Hung Yeh,[b] and Chun-Yen Chang[a]

[a]*Department of Electronics Engineering and Institute of Electronics, National Chiao Tung University, Hsinchu 300, Taiwan*
[b]*NexPower Technology Corporation, Taichung County 421, Taiwan*

Here, double-pattern textured gallium doped zinc oxide (GZO) films were achieved by inserting organosilicon underlayers deposited from an atmospheric pressure plasma jet (APPJ) between sputtered GZO films and glass substrates. The electro-optical characteristics of the textured GZO films were controlled by the haze of organosilicon underlayers. All GZO films were thermally annealed in high vacuum to improve film quality. Post-annealed textured GZO films exhibited an average optical transmittance of about 80% in a wide range. Hall measurements showed Hall mobility above 26 cm^2/V-s, carrier concentration around 2.4×10^{20} cm^{-3} and resistivity below 9.91×10^{-4} Ω-cm.
 [DOI: 10.1149/2.003203ssl]

Manuscript submitted May 29, 2012; revised manuscript received June 19, 2012. Published August 14, 2012.

Transparent conductive oxides (TCO) are essential for superstrate solar cells due to its outstanding optical and electrical properties.[1] In order to improve the efficiency of solar cells, it is important to fabricate high-quality TCO substrates. Recently, zinc oxide (ZnO) based TCO have attracted significant attention because of high abundance, low cost and non-toxicity. Moreover, ZnO films doped with group III elements are more stable than tin-doped indium oxides (ITO) and fluorine-doped tin oxides (FTO) in the hydrogen and silan (SiH_4) plasma discharge.[2,3] Hence, they are very suitable for the process of microcrystalline silicon (μc-Si) and amorphous silicon (a-Si) solar cells.

For silicon based thin film solar cells, textured ZnO electrodes are necessary to increase light absorption in μc-Si absorbers and to reduce the degradation in a-Si absorbers. This is because that textured ZnO films can scatter the incident light efficiently and enhance the light trapping effect. To date, many efforts have been made to achieve superior textured ZnO films. Post wet etching by diluted acids for aluminum-doped zinc oxides (AZO) and gallium-doped zinc oxides (GZO) is the well-known method.[4,5] However, this process creates a lot of waste in ZnO and is not fit for large-scale production. Recently, pyramid-like textured zinc oxides doped with boron (BZO) have been successfully fabricated by a low pressure chemical vapor deposition (LPCVD) or a metal organic chemical vapor deposition (MOCVD) without any post treatments.[6,7] Nevertheless, disadvantages of these techniques are expensive equipments and the usage of toxic precursors.

Here, we developed a novel, safe, and low-cost technique to produce textured GZO films. A bi-layer structure of organosilicon/ GZO was conducted to fabricate double-pattern textured GZO films on glass substrates. This bi-layer structure was achieved by an atmospheric pressure plasma jet (APPJ) and a dc magnetron sputtering. The surface morphology, optical characteristics and conductivity of double-pattern textured GZO films can be effectively controlled by the haze of organosilicon underlayers. After a post-annealing treatment in high vacuum, double-pattern textured GZO films can reveal the excellent optical transmittance and electrical conductivity.

Experimental

The bi-layer structures consisted of organosilicon underlayers and GZO films. The organosilicon underlayers were grown on 10×10 cm^2 Corning Eagle XG glass substrates by a 20 KHz APPJ system and the RF power was 450 W. The temperature of glass substrates were kept at 75°C. The hexamethyldisilazane (HMDSN) precursor was used to deposit the films. Clean dry air (CDA) was the working gas and the flow rate was 40 slm. The distance between the nozzle and the substrate was 15 mm and the nozzle scan speed was 300 mm/s. The Ar carrier gas flow rate [Ar] in APPJ was changed from 120 to 180 sccm to alter the haze of organosilicon films. The 1 μm thick GZO films were deposited on the organosilicon underlayers at 100°C by a dc magnetron sputtering. The ceramic target contained ZnO and 3.2 wt% Ga_2O_3. The dc power density was 3 W/cm^2 and the working pressure was 2 mTorr during the sputtering. Finally, all as-grown textured GZO films were thermally annealed at 500°C in high vacuum ($< 1\times10^{-6}$ torr) for 5 min.

The photoluminescence (PL) measurements were conducted at room temperature (RT) by a He-Cd 325 nm laser to determine the film quality. Optical properties of post-annealed textured GZO films were measured by an UV-Visible-NIR spectrophotometer (Hitachi 4100). Electrical characteristics were examined by Hall measurements in the Van der Pauw configuration at RT. The surface morphology of organosilicon underlayers and textured GZO films were investigated by atomic force microscopy (AFM) and scanning electron microscopy (SEM). X-ray diffraction (XRD) analysis with Cu-K_α radiation was used to study the crystallinity and structure phase in post-annealed textured GZO films.

Results

Figure 1. (inserted figure) shows the SEM pictures of organosilicon underlayers deposited with different [Ar] (120–180 sccm). Here, we purposely created a lot of organosilicon clusters on the glass substrate by an APPJ. During the APPJ deposition, N-H and Si-N bonds of HMDSN were broken easily by the plasma dissociation. Due to the reaction between Si-$(CH_3)_{x\ (x=1\text{-}3)}$ radicals and oxygen from the ambient air, the organosilicon films mainly consisted of Si-O and Si-$(CH_3)_x$ groups.[8] The organosilicon clusters became large and dense with increasing [Ar]. This was because that a great number of active SiO_x-like particles can be produced in the quartz tube near the nozzle under high [Ar].[9] Consequently, these active particles can easily react with each other and form the big clusters on the glass substrate. Here, the haze value was used to quantitatively determine the roughness of organosilicon underlayers[10]

$$Haze = \frac{T_{diffuse}}{T_{total}}, \qquad [1]$$

where the diffuse transmittance ($T_{diffuse}$) and the total transmittance (T_{total}) were measured by a spectrophotometer. The haze value at the wavelength of 550 nm increased from 0.05 to 0.11% with raising [Ar], as shown in Fig. 1.

The surface morphology and cross-section images of double-pattern textured GZO films are shown in Fig. 2. The surface topography was consisted of submicron sized pyramid-like structures and

*Electrochemical Society Student Member.
[z]E-mail: yushuhung1@gmail.com

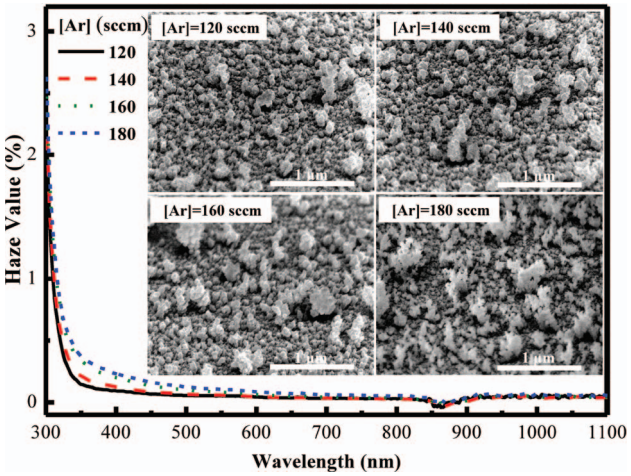

Figure 1. Surface SEM images and haze value of organosilicon underlayers grown under different Ar carrier gas flow rates.

island-like structures. The diameters of island-like shapes ranged between 1 and 1.5 μm. Therefore, double-pattern textured GZO films can effectively scatter the incoming light in the visible and near-infrared region. Here, the organosilicon clusters on the substrates served as the nucleation sites and induced the formation of GZO islands during the sputtering. Hence, the island shapes and grain structure became distinct and big with increasing the roughness of organosilicon underlayers. AFM measurements demonstrated that RMS roughness of textured GZO films can be raised from 29.0 to 54.4 nm with increasing [Ar]. Figure 3 reveals the Hall measurement results of post-annealed textured GZO films as a function of the RMS roughness. The carrier density showed slight variations with increasing the RMS roughness of GZO films. We speculated that the surface roughness of organosilicon underlayers did not obviously affect the activation of Ga atoms and the carrier density in the GZO films. However, Hall mobility suffered a huge impact and decreased from 31.1 to 26.0 cm^2/V-s. This mobility degradation was attributed to both defect scattering and grain boundary scattering in the GZO films. During the sputtering, low surface migration of sputtered atoms on the highly rough organosilicon surface can increase lattice defects in GZO films. Moreover, the resistivity of the GZO films increased from 8.14×10^{-4} to 9.91×10^{-4} Ω-cm accompanying the reduction of the mobility.

Figure 4 shows the RT PL spectra and simulation curves calculated by Gaussian functions of post-annealed textured GZO films. For textured GZO films with the RMS roughness of 29.9 nm, the ultraviolet

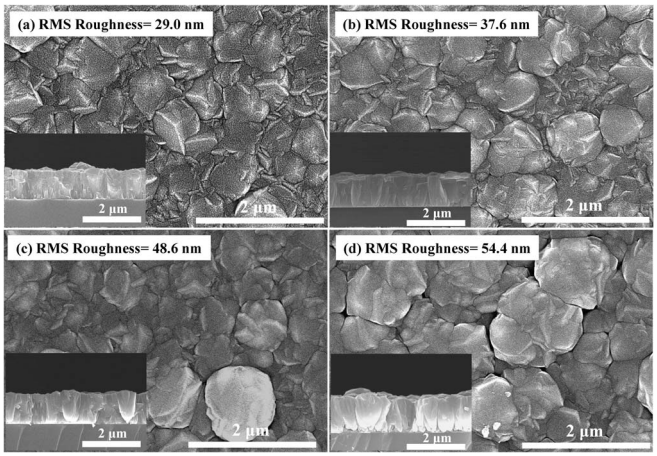

Figure 2. Surface and cross-section SEM images of 1 μm thick textured GZO films. The RMS roughness of textured GZO films was determined by AFM.

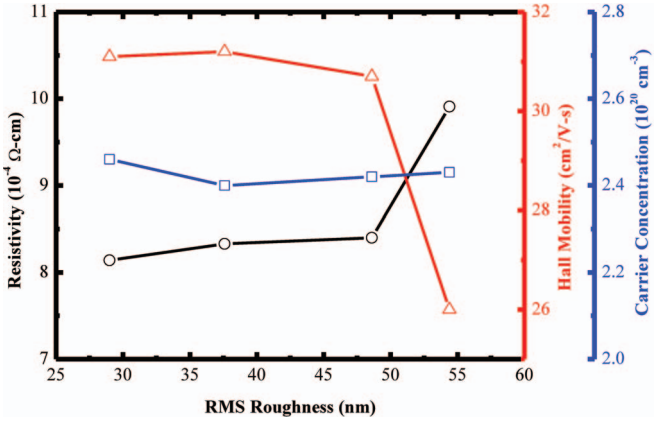

Figure 3. Carrier concentration (□), Hall mobility (△) and resistivity (◯) of post-annealed textured GZO films as the function of RMS roughness.

(UV) emission peaks at 3.35 and 3.22 ev and the blue emission peaks at 2.73 and 2.61 ev were observed. Examine the RT PL spectra of the bare glass (data not shown), the blue emission of 2.73 ev and the UV emission of 3.1 ev were attributed to the composition in glass substrates. The UV emission of 3.35 ev was the typical near-band-edge (NBE) emission generated from free-exciton recombination. The blue emission of 2.61 ev was generated from deep-level emission caused by the impurity and crystal defects. With increasing the RMS roughness

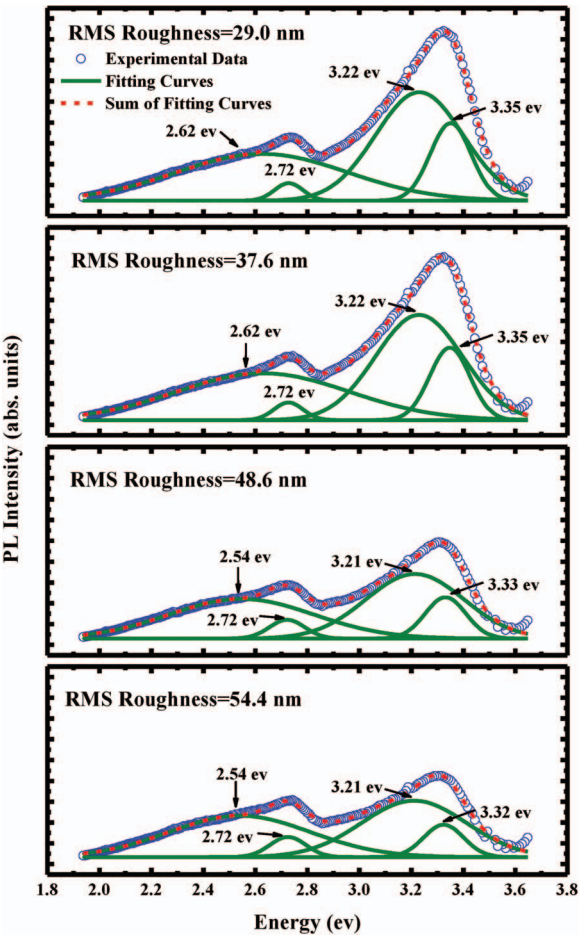

Figure 4. RT PL spectra (symbol), simulation curves (solid line) fitted with Gaussian functions and the sum of fitting curves (dash line) of post-annealed textured GZO films.

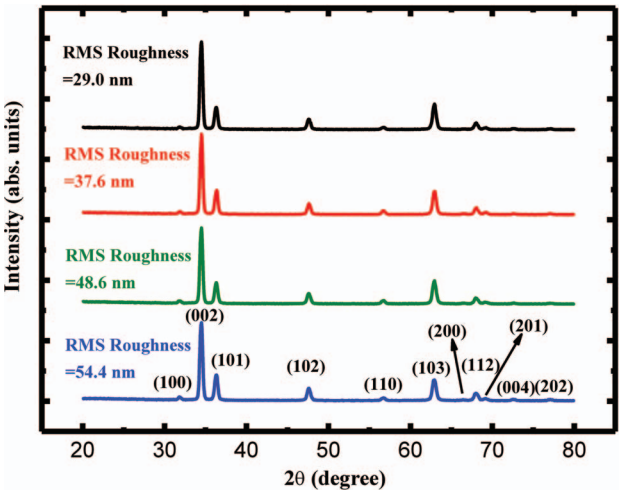

Figure 5. XRD spectra of post-annealed textured GZO films with various RMS roughness values.

of textured GZO films, the NBE emission and deep-level emission revealed a slight red-shift, furthermore, the PL peak intensity from NBE emission was reduced significantly. This phenomenon was attributed to the increase of non-radiative centers. This consequence corresponded to the cause of degraded Hall mobility in highly textured GZO films.

The ZnO films deposited by sputtering are usually polycrystalline with a hexagonal wurtzite structure.[11] Substantially, the preferred growth orientation perpendicular to the substrate is related to the geometric pattern on the textured GZO surface. In order to clarify the relation between preferred orientation and surface morphology in this study, we conducted the XRD measurement. The XRD spectra of post-annealed textured GZO films are shown in Fig. 5. The spectra demonstrated that all textured GZO films had a strong (002) texture growth. This was due to the lowest surface energy of (002) plane in ZnO films.[12] (002) peak intensity did not change significantly with increasing RMS roughness of textured GZO films. In addition to the (002) crystal orientation, the (100), (101), (102), (110), (103), (200), (112), (201), (004) and (202) contributed the geometric profiles to the surface morphology of textured GZO films.

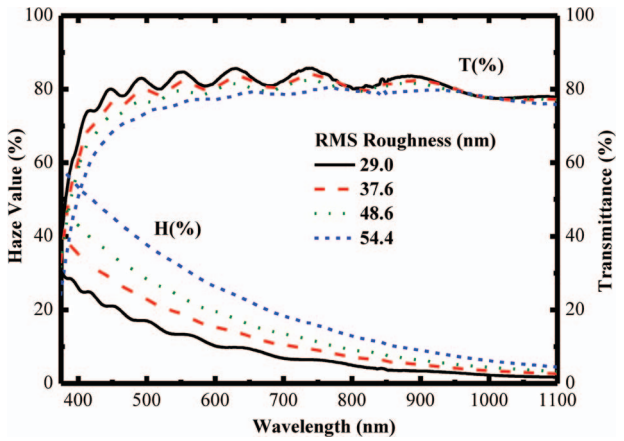

Figure 6. Haze value and optical transmittance spectra of post-annealed GZO films with different RMS roughness values.

Figure 6 illustrates the optical transmittance and the haze value of post-annealed textured GZO films. For most of films, the average transmittance in a wide wavelength range was about 80%. With increasing the RMS roughness, a strong defect absorption in the visible range was observed. This absorption was caused by the optically-assisted electron transfer from valance band to trap states in the forbidden gap.[13] Moreover, the haze value in a wide wavelength range can be enhanced apparently by increasing the RMS roughness of textured GZO films. Here, maximum haze value of 32% at the wavelength of 550 nm was achieved. Due to the enhancement in haze values, the interference phenomenon in the optical transmittance spectra can be decreased significantly also shown in Fig. 6.

Conclusions

The double-pattern textured GZO films with outstanding electro-optical properties were successfully achieved by an AAPJ and a dc sputtering. The organosilicon underlayers with SiO_x-like clusters grown by an APPJ provided nucleation sites and resulted in the formation of submicron sized pyramid-like structures and micron sized island-like structures during the GZO sputtering. With increasing the surface roughness of organosilicon underlayers, the haze value of textured GZO in a wide wavelength range can be enhanced significantly. Furthermore, all post-annealed textured GZO films showed the average optical transmittance about 80% in the range of 400–1100 nm. Although RT PL spectra manifested the increase of structural defects in highly textured GZO films, these films exhibited excellent Hall mobility above 26 cm^2/V-s and resistivity below 9.91×10^{-4} Ω-cm. The benefits of textured GZO fabrication in this investigation include inexpensive manufacture, in situ texturing growth and reduction of material consumption. Therefore, this technique reveals high potential for PV industrial production of transparent conductors.

Acknowledgments

This work was supported by the National Science Council of Taiwan under Grant NSC 101-3113-E-009-004.

References

1. J. Müller, B. Rech, J. Springer, and M. Vanecek, *Sol. Energy*, **77**, 917 (2004).
2. R. Banerjee, S. Ray, N. Basu, A. K. Batabyal, and A. K. Barua, *J. Appl. Phys.*, **62**, 912 (1987).
3. H. Sato, T. Minami, and S. Takata, *J. Vac. Sci. Technol. A*, **11**, 2975 (1993).
4. O. Kluth, B. Rech, L. Houben, S. Wieder, G. Schöpe, C. Beneking, H. Wagner, A. Löffl, and H. W Schock, *Thin Solid Films*, **351**, 247 (1999).
5. H. Jia, T. Matsui, and M. Kondo, *Prog. Photovolt: Res. Appl.*, **20**, 111 (2012).
6. J. Bailat, D. Dominé, R. Schlüchter, J. Steinhauser, S. Faÿ, F. Freitas, C. Bücher, L. Feitknecht, X. Niquille, T. Tscharner, A. Shah, and C. Ballif, in *Conf. Rec. IEEE 4th World Conf. Photovoltaic Energy Convers*, **2**, 1533 (2006).
7. X. L. Chen, B. H. Xu, J. M. Xue, Y. Zhao, C. C. Wei, J. Sun, Y. Wang, X. D. Zhang, and X. H. Geng, *Thin Solid Films*, **515**, 3753 (2007).
8. S. Sahli, S. Rebiai, P. Raynaud, Y. Segui, A. Zenasni, and S. Mouissat, *Plasmas Polym.*, **7**, 327 (2002).
9. Shih-Hsien Yang, Chi-Hung Liu, Chun-Hsien Su, and Hui Chen, *Thin Solid Films*, **517**, 5284 (2009).
10. W. T. Yen, Y. C. Lin, and J. H. Ke, *Appl. Surf. Sci.*, **257**, 960 (2010).
11. P. F. Carcia, R. S. McLean, M. H. Reilly, and G. Nunes Jr., *Appl. Phys. Lett.*, **82**, 1117 (2003).
12. N. Fujimura, T. Nishihara, S. Goto, J. Xu, and T. Ito, *J. Cryst. Growth* **130**, 269 (1993).
13. S. Adachi, *Optical properties of crystalline and amorphous semiconductor, materials and fundamental principles*, Kluwer academic publishers, London, (1999).